Neuroradiology (2004) 46: 628–634
DOI 10.1007/s00234-004-1239-6

T. Satoh
C. Ekino
C. Ohsako

Transluminal color-coded three-dimensional magnetic resonance angiography for visualization of signal Intensity distribution pattern within an unruptured cerebral aneurysm: preliminarily assessment with anterior communicating artery aneurysms

Received: 28 October 2003
Accepted: 20 April 2004
Published online: 8 July 2004

T. Satoh (✉)
Department of Neurological Surgery,
Ryofukai Satoh Neurosurgical Hospital,
5-23-23 Matsunaga, Fukuyama,
729-0104 Hiroshima, Japan
E-mail: ucsfbtrc@urban.ne.jp
Tel.: +84-934-9911
Fax: +84-934-9910

C. Ekino · C. Ohsako
Diagnostic Radiology, Ryofukai Satoh
Neurosurgical Hospital, Hiroshima, Japan

Abstract The natural history of unruptured cerebral aneurysm is not known; also unknown is the potential growth and rupture in any individual aneurysm. The authors have developed transluminal color-coded three-dimensional magnetic resonance angiography (MRA) obtained by a time-of-flight sequence to investigate the interaction between the intra-aneurysmal signal intensity distribution patterns and configuration of unruptured cerebral aneurysms. Transluminal color-coded images were reconstructed from volume data of source magnetic resonance angiography by using a parallel volume-rendering algorithm with transluminal imaging technique. By selecting a numerical threshold range from a signal intensity opacity chart of the three-dimensional volume-rendering dataset several areas of signal intensity were depicted, assigned different colors, and visualized transparently through the walls of parent arteries and an aneurysm. Patterns of signal intensity distribution were analyzed with three operated cases of an unruptured anterior communicating artery aneurysm and compared with the actual configurations observed at microneurosurgery. A little difference in marginal features of an aneurysm was observed; however, transluminal color-coded images visualized the complex signal intensity distribution within an aneurysm in conjunction with aneurysmal geometry. Transluminal color-coded three-dimensional magnetic resonance angiography can thus provide numerical analysis of the interaction between spatial signal intensity distribution patterns and aneurysmal configurations and may offer an alternative and practical method to investigate the patient-specific natural history of individual unruptured cerebral aneurysms.

Keywords Computer visualization · Intra-aneurysmal flow · Intracranial aneurysm · Magnetic resonance angiography · Signal intensity distribution

Introduction

Because the natural history of an unruptured cerebral aneurysm is not known, the interaction between the intra-aneurysmal blood flow and morphological features of the aneurysmal geometry has been studied to elucidate the potential growth and rupture of an unruptured cerebral aneurysm [1, 2, 3, 4, 5, 6, 7, 8, 9]. Current advances in magnetic resonance angiography (MRA) provide us with serial fine volume data of the aneurysmal angioarchitecture, including parent arteries and an aneurysm [10, 11, 12, 13]. MRA signals obtained by a time-of-flight (TOF) sequence may provide noninvasive and feasible interpretation of the blood flow information within an aneurysm [1, 14, 15, 16, 17, 18]. A postprocessing numerical analysis of the MRA dataset can

visualize three-dimensional (3D) distribution of MR signal intensities. Additionally, specific areas of signals can be selected from the dataset of the MR signal intensity opacity chart using a functional curve with certain threshold ranges and assigned different colors.

The authors have developed transluminal color-coded 3D MRA to investigate the interaction between the signal intensity distribution patterns and configuration of unruptured cerebral aneurysms. In the present study transluminal color-coded images of the 3D MRA were applied in three operated cases of an unruptured anterior communicating artery aneurysm. Compared with the actual outer-wall configurations observed at microneurosurgery, the spatial signal intensity distribution patterns of transluminal color-coded images of 3D MRA were assessed with respect to the aneurysmal geometry.

Materials and methods

MRA data acquisition

We studied three cases with an unruptured anterior communicating artery aneurysm detected incidentally at MRA, including one case resulting in rupture with time course. MRA was performed with 1.0-T equipment (Signa HiSpeed; GE Medical Systems, Milwaukee, Wis., USA). Images were obtained with a 3D TOF, spoiled gradient-recalled acquisition in the steady state sequence, without cardiac or respiratory gating. Imaging protocol was as follows: 35/3.9–4.1/2 (TR/TE/excitations), flip angle 20°, 192×128 matrix, 1.2-mm thickness, 0.6-mm slice interval, 16-cm field of view, without magnetization transfer contrast, total imaging time 8 min 49 s (two slabs), 60 sections in total (two slabs), zero-fill interpolation processing two times, overlap of eight sections. A total of 104 source axial volume data were obtained and were transferred to a workstation with computer medical visualization software (Zio M900; AMIN, Tokyo, Japan).

Transluminal color-coded images of 3D MRA

The workstation interpolated the data every 0.3 mm and processed the results into a 3D volume-rendering dataset (207 data) in 9 s. The transluminal color-coded 3D MRA images were rendered from the dataset in 11 s using a parallel volume-rendering algorithm with a transluminal imaging technique [1, 19, 20]. Based on a histogram of the signal intensity distribution corresponding to the luminal margin on the source volume data, transparency of the luminal wall was selected from the opacity chart of MR signal intensities (arbitrary units distribution) by using a function of spiked peak curve with a threshold range of 155–165 (peak value at 160 with 100% opacity level, window width 10). Those transluminal images represented the contour of the parent arteries and an aneurysm as a series of rings, and color-rendered in red-purple.

To create transparent visualization of intraluminal volume data through the vessel wall other square curves were employed to select several specific areas of signal intensity serially from the same opacity chart used for the transluminal images. These areas were extracted with threshold ranges of 200–250 (10% opacity level), 250–300 (20% opacity level), and 300–500 (30% opacity level) and were color-coded blue, green, and red, respectively. The color-coded signal intensity areas were superimposed onto the tranluminal images to create computer-generated transluminal color-coded images and were shown separately with each threshold range on several 3D images or altogether on a single 3D image. The total time required producing each transparent color-coded images of 3D MRA was approximately 20 s from post-MR scanning.

Transluminal color-coded 3D MRA was reconstructed retrospectively through the similar projections as to the operative views. Intraoperative findings of the actual outer-wall features, including neck complex, bulging and bleb of the sac, and perianeurysmal structures were compared with those of the projection matched transluminal color-coded images of 3D MRA.

Results

With the transluminal color-coded images intraluminal information of MRA was color-coded and depicted three-dimensionally with respect to the contours of the parent arteries and an aneurysm. The 3D distribution of signal intensity within each individual aneurysm was shown as an area with different colors and projected in various directions. Compared with the intraoperative findings, a little discrepancy in marginal features of an aneurysm was observed between 3D MRA and the actual intraoperative features.

Case 1

A 60-year-old man had an incidentally discovered unruptured anterior communicating artery aneurysm. The volume-rendering image of 3D MRA (Fig. 1A), right anterior projection, showed the aneurysm (6.7×6.7×5.9 mm in size) with a blunt dome at the left lateral tip of the sac (arrows), a gentle ridge along the anterior aspect of the sac terminated to a slight bulging near the neck (arrowheads). Those features were slightly different but fundamentally consistent with the operative findings (Fig. 1B). The transluminal color-coded flow

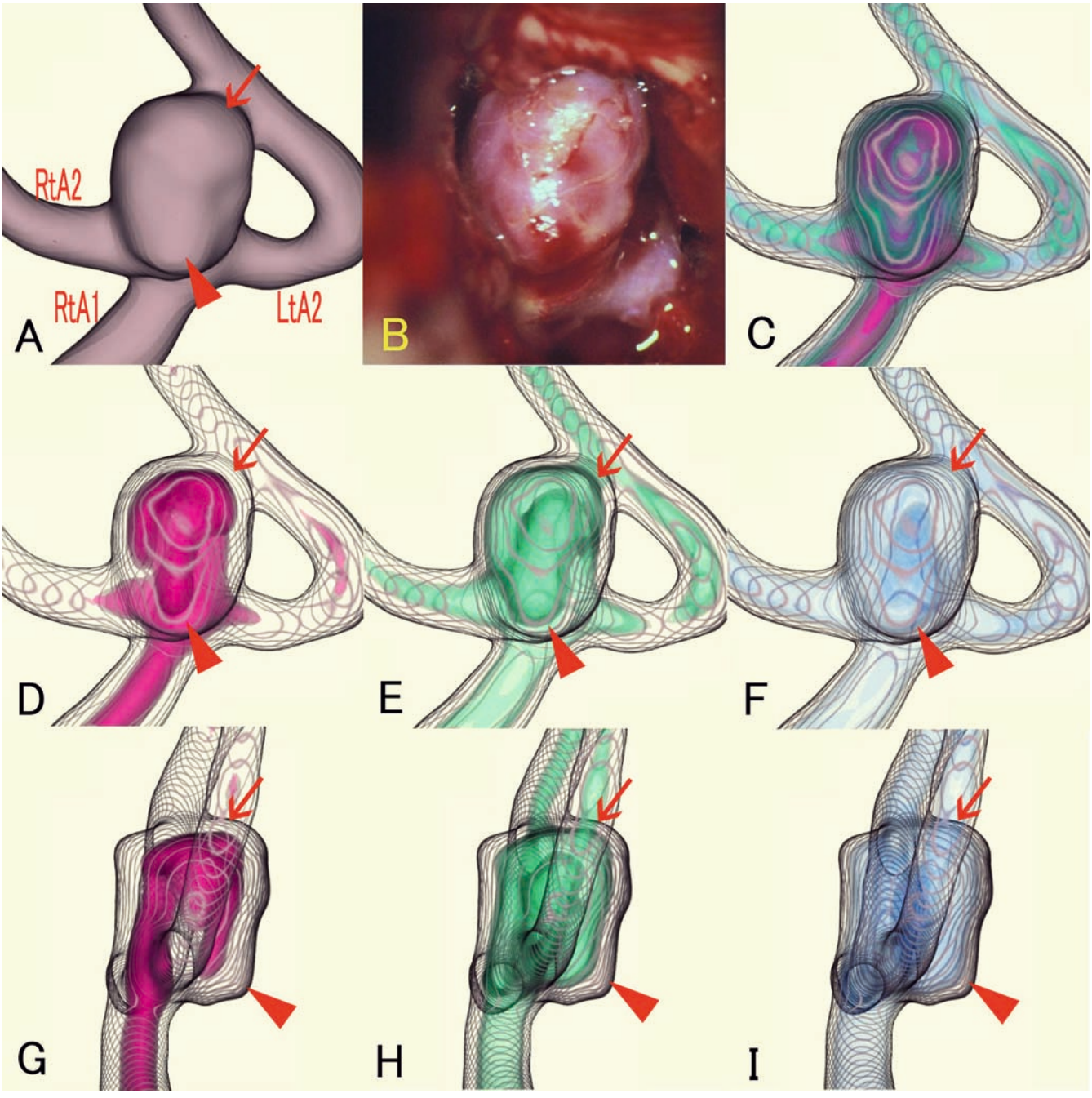

Fig. 1 Case 1: a 60-year-old man with an unruptured anterior communicating artery aneurysm. **A** Volume-rendering 3D MRA, right anterior projection. *Arrows* Blunt dome at the left lateral tip; *arrowheads* bulging of the sac. **B** Operative photo; similar projection. **C** Transluminal color-coded flow images of 3D MRA with mixed red, green, and blue colors altogether; right anterior projection. **D–F**, **G–I** Transluminal color-coded flow images of 3D MRA selected by signal intensity threshold range of 300–500 (*red*), 250–300 (*green*), and 200–250 (*blue*). **D–F** Right anterior projections. **G–I** Right lateral) projections

images showed flow patterns with colors altogether on a single 3D image (Fig. 1C) or different colors separately, according to the threshold ranges, on several 3D images from various projections (Fig. 1D–F, G–I). The distribution pattern of signal intensity was interpreted as follows: In the direction of the afferent right anterior cerebral artery (A1) the profound high signal intensity area was observed at the backside of the neck orifice along the posterior wall extended to the dome at the tip and projected back along the ridge of the anterior aspect of the sac. Areas with relatively high and slightly high

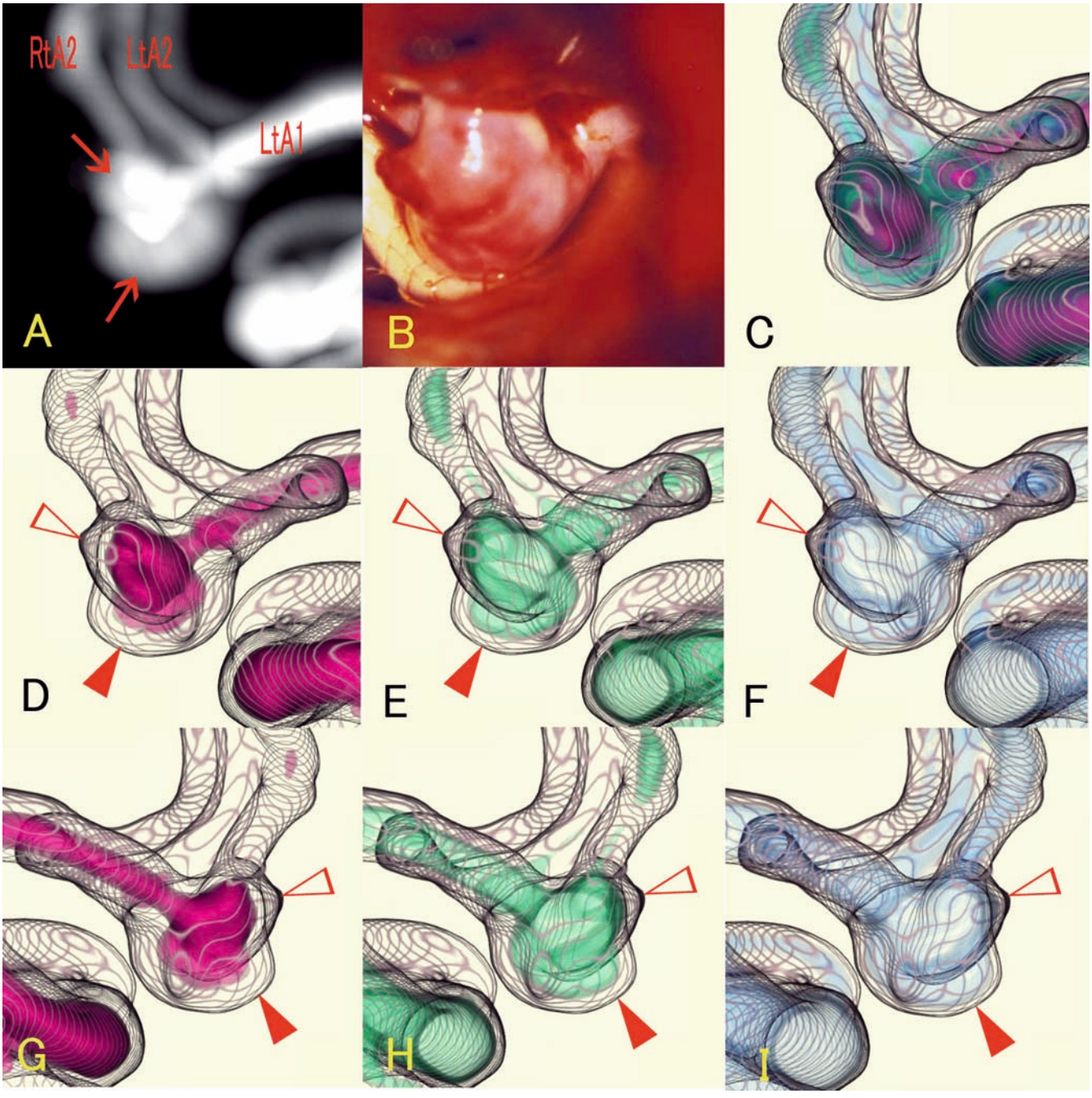

Fig. 2 Case 2: a 56-year-old man with an unruptured anterior communicating artery aneurysm. **A** Maximum intensity projection image of MRA; right inferoanterior projection. *Arrows* Superior and inferior domes. **B** Operative photo; similar projection. **C** Transluminal color-coded flow images of 3D MRA with mixed red, green, and blue colors altogether; right inferoanterior projection. **D–F**, **G–I** Transluminal color-coded flow images of 3D MRA selected by signal intensity threshold range of 300–500 (*red*), 250–300 (*green*), and 200–250 (*blue*). **D–F** Right inferoanterior projections. **G–I** Right inferoposterior projections. *Filled arrowheads* Margin of the inferior dome; *unfilled arrowheads* tip of the superior dome

signal intensity distribution were observed at the central zone and beneath the bulging at the frontal sac adjacent to the neck (arrowheads).

Case 2

A 56-year-old man had an unruptured anterior communicating artery aneurysm showing an episode of transient visual field defect. The maximum intensity projection image of MRA (Fig. 2A), right inferoanterior

projection, showed the aneurysm (6.8×6.7×4.9 mm in size) with superior and inferior domes (arrows). The actual contours of the aneurysm at the operation (Fig. 2B) were similar to but differed slightly from those of MRA, showing the superior dome with a sharp tip at the right superolateral wall, and the inferior dome expanded roundly and embedded into the left optic nerve and chiasm. With transluminal color-coded images (Fig. 2C, D–F, G–I) the signal intensity distribution pattern was interpreted as follows: The profound high signal intensity area was observed at the aneurysmal ostium in a direction of the dominant left A1, and along to the superior dome. A relatively high signal intensity area was observed along the wall of the inferior dome, and slightly high signal intensity area along the margin of the inferior dome (arrowheads) and beneath the tip of the superior dome (white arrowheads).

Case 3

An 83-year-old woman had an unruptured anterior communicating artery aneurysm and resulted in rupture 3 months after MRA. The volume-rendering 3D MRA (Fig. 3A) and the maximum intensity projection image (Fig. 3B), right inferoanterior projection, 3 months before rupturing showed the aneurysm (7.2×5.0×10.3 mm in size) with two large domes (arrows) extended superposteriorly and inferoanteriorly. With the transluminal color-coded images (Fig. 3C, D–F) the signal intensity distribution pattern was interpreted as follows: the high signal intensity area was observed along the afferent left A1 to the aneurysmal orifice and efferent left A2, and extended beneath the superoposterior dome. The relatively high signal intensity area was observed at the inferoanterior dome (arrowheads). The slightly high signal intensity area was shown at the inferoanterior dome adjacent to the anterior aspect of the neck (white arrowheads). Serial 3D computed tomography angiographies performed 7 months (Fig. 3G) and 5 months (Fig. 3H) before rupturing, and at the time of rupture (Fig. 3I) showed the morphological change in the aneurysmal configuration. The inferior dome (arrowheads) expanded slightly in the first 2 months (Fig. 3H) and then grew anteroinferior direction at the time of rupture 7 months later (Fig. 3I). Retrospectively, the change in shape during follow-up time course was observed at the anteroinferior wall of the sac (arrowheads, white arrowheads), and which corresponded to the area with relatively and slightly high signal intensity distribution shown by the transluminal color-coded 3D MRA 3 months before rupturing (Fig. 3C, D–F). The patient was operated on and successfully clipped the next day. No thrombus or calcification was observed within the aneurysm, but the exact and precise ruptured point of the sac was not identified during the microneurosurgery.

Fig. 3 Case 3: an 83-year-old woman with an unruptured anterior communicating artery aneurysm resulting in rupture. **A** Volume-rendering 3D MRA; right inferoanterior projection. *Arrows* Two large domes. **B** Maximum intensity projection image of MRA; right inferoanterior projection. **C** Transluminal color-coded flow images of 3D MRA scanned 3 months before rupturing, with mixed red, green, and blue colors altogether; right inferoanterior projection. **D–F** Transluminal color-coded flow images of 3D MRA selected by signal intensity threshold range of 300–500 (*red*), 250–300 (*green*), and 200–250 (blue); right inferoanterior projection. *Filled arrowheads* Relatively high signals at the inferoanterior dome; *unfilled arrowheads* slightly high signals at the area adjacent to the neck. **G–I** Serial 3D computed tomography angiographic images 7 months (**G**) and 5 months (**H**) before rupturing and at the time of rupture (**I**); right inferoanterior projection. *Filled arrowheads* Inferior dome; *unfilled arrowheads* anteroinferior dome

Discussion

MRA is a noninvasive technique to obtain vessels-to-soft tissue contrast by the flow of the spins within the blood vessels [14, 15]. The inflow effect on TOF MRA sequence causes flow void related mainly to peak inflow velocity within the vessel lumen during data acquisition process through the diastolic and systolic cardiac cycles [1, 14, 15, 16]. The signal intensity of each pixel appeared on the source images can provide flow related information, but with oversimplified actual flow [1]. The magnitude of signal intensity is complicated and affected by several factors. Loss of signals occurs mainly by spin saturation phenomenon due to slow flow, phase dispersion due to disturbed and complex flow (turbulent flow, acceleration, pulsation, and higher order motion), and susceptibility or partial volume effects [1, 14, 15, 16, 17]. Depending on the aneurysmal geometry, including the size of the neck and the flow ratio in distal branches, complex intra-aneurysmal flow phenomena are generated by circulating flow, recirculating flow, and stagnation or stasis of flow [1, 2, 3, 4, 7, 8, 18]. Complex or disturbed flow conditions within the aneurysm may cause a decrease in signal intensity. Additionally, because the flow within aneurysms varies in complexity according to pulsation, intra-aneurysmal flow may change with variations in heart rate [1, 12]. Interpretation of signals of TOF MRA requires careful consideration of potential pitfalls appeared on the volume data of source images. In general, the bright pixels may be assigned to high flow velocity, but the darker pixels may not indicate low flow velocity. It is not feasible to assign and quantify the magnitude of signal

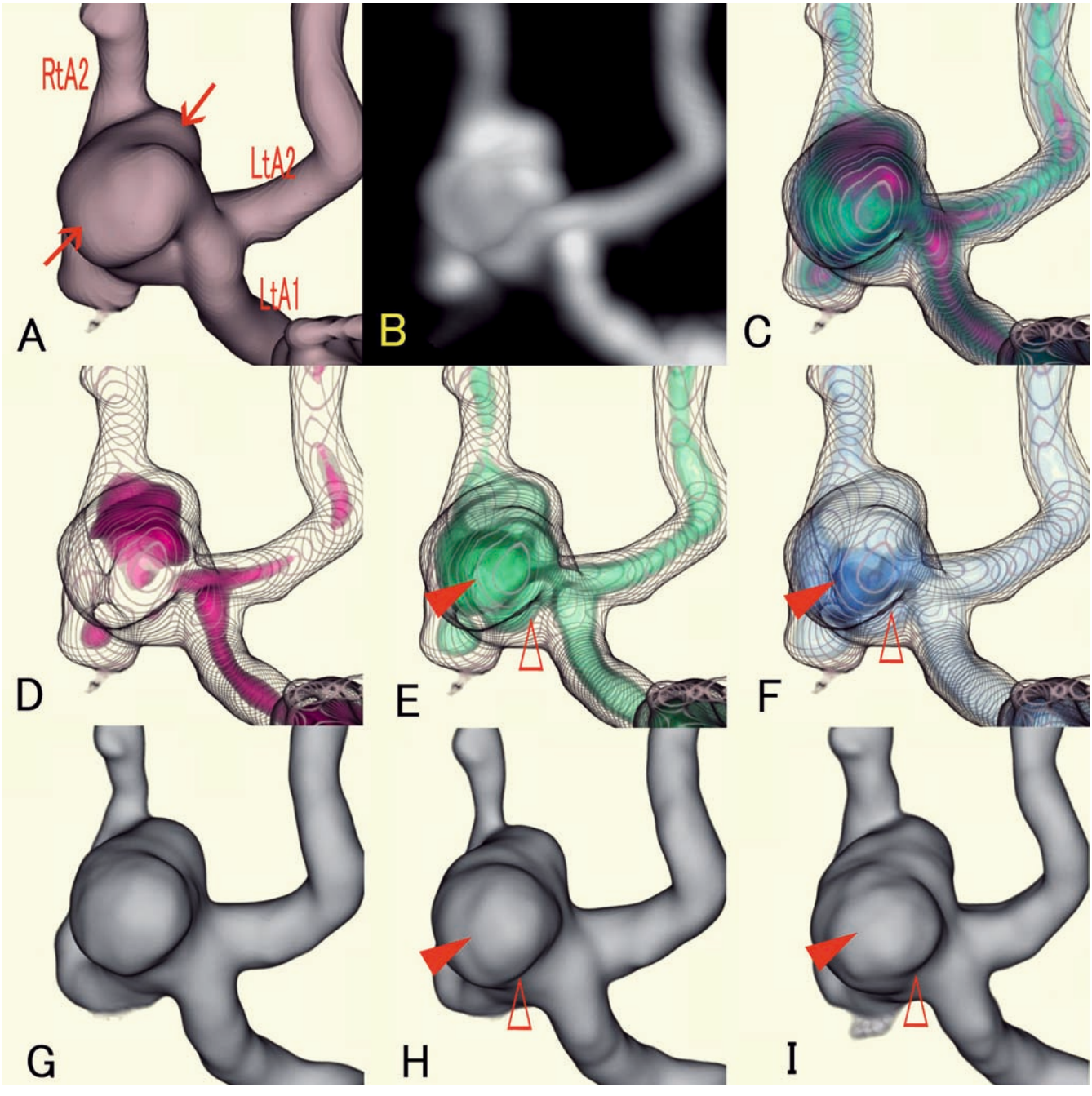

intensity to the actual flow velocity, however, complex and disturbed flow conditions within an aneurysm may be depicted as an area with relatively low signal intensity distribution on TOF MRA.

A postprocessing computer medical visualization software offers numerical imaging analysis of the 3D reconstructed volume-rendering dataset and then depicts the specific results as a computer-generated 3D image. Transluminal imaging reconstruction technique provides transparent visualization of the intraluminal volume data through the vessel wall, so that the signal intensity distribution of MRA obtained by TOF sequence can be depicted three-dimensionally [1, 19, 20]. The transluminal flow images of 3D MRA interpret the intra-aneurysmal flow patterns as a change in signal intensity by the animated display but without temporal information of actual flow dynamics [1]. As shown in the present study, the transluminal color-coded images can visualize spatial signal intensity distribution within an aneurysm, with different colors assigning to the numerical thresh-

old ranges and opacity levels of signal intensities. With the transparent color-coded images of 3D MRA the relationship between the signal intensity distribution and the corresponding aneurysmal geometry, including neck complex, bulging dome, and bleb, can be assessed three-dimensionally from various projections.

The transluminal color-coded 3D MRA is a visually appealing and informative means of postprocessing and displaying TOF MRA. These images may allow us to follow-up the patient-specific natural history of each individual unruptured cerebral aneurysm with time course. Further studies investigating the effect of magnitude and distribution of intra-aneurysmal signals on the natural history of various unruptured cerebral aneurysms are necessary.

Conclusions

The transluminal color-coded images of 3D MRA can provide a practical and prospective method to investigate the patient-specific natural history of each individual unruptured cerebral aneurysm with respect to the interaction between the intra-aneurysmal signal intensity distribution and the aneurysmal angioarchitecture. More work is required to validate the technique in unruptured aneurysms with various locations and ruptured cases of previously unruptured aneurysms. Additionally, comparison of the color-coded images with the actual aneurysmal configurations observed at microneurosurgeries or intraluminal dynamics of contrast agent obtained during interventional procedures is necessary.

References

1. Satoh T, Onoda K, Tsuchimoto S (2003) Visualization of intraaneurysmal flow patterns with transluminal flow images of 3D MR angiograms in conjunction with aneurysmal configurations. AJNR Am J Neuroradiol 24:1436–1445
2. Steinman DA, Milner JS, Norley CJ, Lownie SP, Holdsworth DW (2003) Image-based computational simulation of flow dynamics in a giant intracranial aneurysm. AJNR Am J Neuroradiol 24:559–566
3. Gailloud P, Khan HG, Albayram S, Martin J-B, Rufenacht DA, Murphy KJ (2002) Pooling of echographic contrast agents during transcranial Doppler sonography: a sign in favor of slow-flowing giant saccular aneurysms. Neuroradiology 44:21–24
4. Ujiie H, Tachibana H, Hiramatsu O, Hazel AL, Matsumoto T, Ogasawara Y, Nakajima H, Hori T, Takakura K, Kajiya F (1999) Effects of size and shape (aspect ratio) on the hemodynamics of saccular aneurysms: a possible index for surgical treatment of intracranial aneurysms. Neurosurgery 45:199–130
5. Kerber CW, Imbesi SG, Knox K (1999) Flow dynamics in a lethal anterior communicating artery aneurysm. AJNR Am J Neuroradiol 20:2000–2003
6. Takeshima S, Murayama Y, Villablanca P, Morino T, Nomura K, Tanishita K, Vinuela F (2003) In vitro measurement of fluid-induced wall shear stress in unruptured cerebral aneurysms harboring blebs. Stroke 34:187–192
7. Steiger HJ, Poll A, Liepsch D, Reulen HJ (1987) Basic flow structure in saccular aneurysm: a flow visualization study. Heart Vessels 3:55–56
8. Gobin YP, Counord JL, Flaud P, Duffaux J (1994) In vitro study of haemodynamics in a giant saccular aneurysm model: influence of flow dynamics in the parent vessel and effects of coil embolization. Neuroradiology 36:530–536
9. Burleson AC, Strother CM, Turitto VT (1995) Computer modeling of intracranial saccular and lateral aneurysms for the study of their hemodynamics. Neurosurgery 37:774–784
10. Korogi Y, Takahashi M, Mabuchi N, Miki H, Fujiwara S, Horikawa Y, Nakagawa T, O'Uchi T, Watabe T, Shiga H, Furuse M (1994) Intracranial aneurysms: diagnostic accuracy of three-dimensional, Fourier transform, time-of-flight MR angiography. Radiology 193:181–186
11. Maeder PP, Weuli RA, de Tribolet N (1996) Three-dimensional volume rendering for magnetic resonance angiography in the screening and preoperative workup of intracranial aneurysms. J Neurosurg 85:1050–1055
12. Adams WM, Laitt RD, Jackson A (2000) The role of MR angiography in the pretreatment assessment of intracranial aneurysms: a comparative study. AJNR Am J Neuroradiol 21:1618–1628
13. Mallouhi A, Chemelli A, Judmaier W, Giacomuzzi S, Jaschke WR, Waldenberger P (2002) Investigation of cerebrovascular disease with MR angiography: comparison of volume rendering and maximum intensity projection algorithms-initial assessment. Neuroradiology 44:961–967
14. Sevick RJ, Tsuruda JS, Schmalbrock P (1990) Three-dimensional time-of-flight MR angiography in the evaluation of cerebral aneurysms. J Comput Assist Tomogr 14:874–881
15. Bosmans H, Wilms G, Marchal G, Demaerel P, Baert AL (1995) Characterization of intracranial aneurysms with MR angiography. Neuroradiology 37:262–266
16. Wilcock DJ, Jaspan T, Worthington BS (1995) Problems and pitfalls of 3-D TOF magnetic resonance angiography of the intracranial circulation. Clin Radiol 50:526–532
17. Piotin M, Gailloud P, Bidaut L, Mandai S, Muster M, Moret J, Rufenacht DA (2003) CT angiography, MR angiography and rotational digital subtraction angiography for volumetric assessment of intracranial aneurysms. an experimental study. Neuroradiology 45:404–409
18. Jager HR, Ellamushi H, Moore EA, Grieve JP, Kitchen ND, Taylor WJ (2000) Contrast-enhanced MR angiography of intracranial giant aneurysms. AJNR Am J Neuroradiol 21:1900–1907
19. Satoh T (2001) Transluminal imaging with perspective volume rendering of computed tomographic angiography for the delineation of cerebral aneurysms. Neurol Med Chir (Tokyo) 41:425–430
20. Satoh T, Onoda K, Tsuchimoto S (2003) Intraoperative evaluation of aneurysmal architecture: comparative study with transluminal images of 3D MR and CT angiograms. AJNR Am J Neuroradiol 24:1975–1981